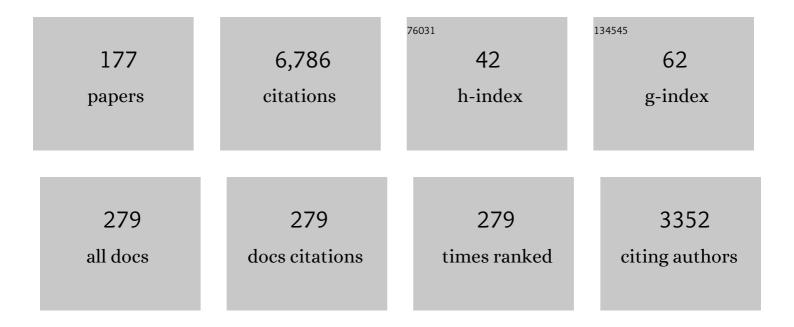
List of Publications by Year in descending order

Source: https://exaly.com/author-pdf/4394707/publications.pdf Version: 2024-02-01



#	Article	IF	CITATIONS
1	Design and description of the MUSICA IASI full retrieval product. Earth System Science Data, 2022, 14, 709-742.	3.7	8
2	Challenge of modelling GLORIA observations of upper troposphere–lowermost stratosphere trace gas and cloud distributions at high latitudes: a case study with state-of-the-art models. Atmospheric Chemistry and Physics, 2022, 22, 2843-2870.	1.9	0
3	Biomass burning pollution in the South Atlantic upper troposphere: GLORIA trace gas observations and evaluation of the CAMS model. Atmospheric Chemistry and Physics, 2022, 22, 3675-3691.	1.9	3
4	Remotely Sensed Carbonyl Sulfide Constrains Model Estimates of Amazon Primary Productivity. Geophysical Research Letters, 2022, 49, .	1.5	7
5	High-resolution optical constants of crystalline ammonium nitrate for infrared remote sensing of the Asian Tropopause Aerosol Layer. Atmospheric Measurement Techniques, 2021, 14, 1977-1991.	1.2	3
6	Observation of cirrus clouds with GLORIA during the WISE campaign: detection methods and cirrus characterization. Atmospheric Measurement Techniques, 2021, 14, 3153-3168.	1.2	5
7	Pollution trace gases C <sub>2</sub> H <sub>6</sub> , C <sub>2</sub> H <sub>2</sub> , HCOOH, and PAN in the North Atlantic UTLS: observations and simulations. Atmospheric Chemistry and Physics, 2021, 21,	1.9	6
8	Polar Stratospheric Clouds: Satellite Observations, Processes, and Role in Ozone Depletion. Reviews of Geophysics, 2021, 59, e2020RG000702.	9.0	49
9	Retrieval of Water Vapour Profiles from GLORIA Nadir Observations. Remote Sensing, 2021, 13, 3675.	1.8	1
10	Modeling the Sulfate Aerosol Evolution After Recent Moderate Volcanic Activity, 2008–2012. Journal of Geophysical Research D: Atmospheres, 2021, 126, e2021JD035472.	1.2	7
11	The Michelson Interferometer for Passive Atmospheric Sounding global climatology of BrONO <sub>2</sub> 2002–2012: a test for stratospheric bromine chemistry. Atmospheric Chemistry and Physics, 2021, 21, 18433-18464.	1.9	1
12	First Detection of a Brief Mesoscale Elevated Stratopause in Very Early Winter. Geophysical Research Letters, 2020, 47, e2019GL086751.	1.5	4
13	Solid Ammonium Nitrate Aerosols as Efficient Ice Nucleating Particles at Cirrus Temperatures. Journal of Geophysical Research D: Atmospheres, 2020, 125, e2019JD032248.	1.2	15
14	Pollution trace gas distributions and their transport in the Asian monsoon upper troposphere and lowermost stratosphere during the StratoClim campaign 2017. Atmospheric Chemistry and Physics, 2020, 20, 14695-14715.	1.9	8
15	Technical note: Lowermost-stratosphere moist bias in ECMWF IFS model diagnosed from airborne GLORIA observations during winter–spring 2016. Atmospheric Chemistry and Physics, 2020, 20, 15379-15387.	1.9	5
16	Cirrus cloud shape detection by tomographic extinction retrievals from infrared limb emission sounder measurements. Atmospheric Measurement Techniques, 2020, 13, 7025-7045.	1.2	3
17	Exploration of machine learning methods for the classification of infrared limb spectra of polar stratospheric clouds. Atmospheric Measurement Techniques, 2020, 13, 3661-3682.	1.2	2
18	Ammonium nitrate particles formed in upper troposphere from ground ammonia sources during Asian monsoons. Nature Geoscience, 2019, 12, 608-612.	5.4	95

#	Article	IF	CITATIONS
19	Unusual chlorine partitioning in the 2015/16 Arctic winter lowermost stratosphere: observations and simulations. Atmospheric Chemistry and Physics, 2019, 19, 8311-8338.	1.9	10
20	Sampling bias adjustment for sparsely sampled satellite measurements applied to ACE-FTS carbonyl sulfide observations. Atmospheric Measurement Techniques, 2019, 12, 2129-2138.	1.2	5
21	3-D tomographic limb sounder retrieval techniques: irregular grids and Laplacian regularisation. Atmospheric Measurement Techniques, 2019, 12, 853-872.	1.2	6
22	Nitrification of the lowermost stratosphere during the exceptionally cold Arctic winter 2015–2016. Atmospheric Chemistry and Physics, 2019, 19, 13681-13699.	1.9	6
23	Vortexâ€Wide Detection of Large Aspherical NAT Particles in the Arctic Winter 2011/12 Stratosphere. Geophysical Research Letters, 2019, 46, 13420-13429.	1.5	5
24	MIPAS observations of volcanic sulfate aerosol and sulfur dioxide in the stratosphere. Atmospheric Chemistry and Physics, 2018, 18, 1217-1239.	1.9	24
25	A climatology of polar stratospheric cloud composition between 2002 and 2012 based on MIPAS/Envisat observations. Atmospheric Chemistry and Physics, 2018, 18, 5089-5113.	1.9	38
26	Comparison of ECHAM5/MESSy Atmospheric Chemistry (EMAC) simulations of the Arctic winter 2009/2010 and 2010/2011 with Envisat/MIPAS and Aura/MLS observations. Atmospheric Chemistry and Physics, 2018, 18, 8873-8892.	1.9	15
27	The MIPAS/Envisat climatology (2002–2012) of polar stratospheric cloud volume density profiles. Atmospheric Measurement Techniques, 2018, 11, 5901-5923.	1.2	5
28	Mesoscale fine structure of a tropopause fold over mountains. Atmospheric Chemistry and Physics, 2018, 18, 15643-15667.	1.9	15
29	Aerosols and Water Ice in Jupiter's Stratosphere from UV-NIR Ground-based Observations. Astronomical Journal, 2018, 156, 169.	1.9	7
30	Evaluation of MUSICA IASI tropospheric water vapour profiles using theoretical error assessments and comparisons to GRUAN Vaisala RS92 measurements. Atmospheric Measurement Techniques, 2018, 11, 4981-5006.	1.2	17
31	Airborne limb-imaging measurements of temperature, HNO⁢sub>3⁢/sub>, O <sub>3</sub> , ClONO <sub>2</sub> , H <sub>2</sub> O and CFC-12 during the Arctic winter 2015/2016: characterization, inAsitu validation and comparison to Aura/MLS. Atmospheric Measurement	1.2	23
32	The role of sulfur dioxide in stratospheric aerosol formation evaluated by using in situ measurements in the tropical lower stratosphere. Geophysical Research Letters, 2017, 44, 4280-4286.	1.5	16
33	Impacts of meteoric sulfur in the Earth's atmosphere. Journal of Geophysical Research D: Atmospheres, 2017, 122, 7678-7701.	1.2	10
34	Stratospheric aerosol data records for the climate change initiative: Development, validation and application to chemistry-climate modelling. Remote Sensing of Environment, 2017, 203, 296-321.	4.6	20
35	Diurnal variations of BrONO <sub>2</sub> observed by MIPAS-B at midlatitudes and in the Arctic. Atmospheric Chemistry and Physics, 2017, 17, 14631-14643.	1.9	3
36	Global carbonyl sulfide (OCS) measured by MIPAS/Envisat during 2002–2012. Atmospheric Chemistry and Physics, 2017, 17, 2631-2652.	1.9	25

#	Article	IF	CITATIONS
37	Denitrification, dehydration and ozone loss during the 2015/2016 Arctic winter. Atmospheric Chemistry and Physics, 2017, 17, 12893-12910.	1.9	35
38	MIPAS IMK/IAA CFC-11 (CCl <sub>3</sub> F) and CFC-12 (CCl <sub>2</sub> F <sub>2</sub> ) measurements: accuracy, precision and long-term stability. Atmospheric Measurement Techniques, 2016, 9, 3355-3389.	1.2	15
39	Monsoon circulations and tropical heterogeneous chlorine chemistry in the stratosphere. Geophysical Research Letters, 2016, 43, 12,624.	1.5	23
40	First detection of ammonia (NH <sub>3</sub> ) in the Asian summer monsoon upper troposphere. Atmospheric Chemistry and Physics, 2016, 16, 14357-14369.	1.9	51
41	Measurements of global distributions of polar mesospheric clouds during 2005–2012 by MIPAS/Envisat. Atmospheric Chemistry and Physics, 2016, 16, 6701-6719.	1.9	10
42	Spectroscopic evidence of large aspherical <i>β</i> -NAT particles involved in denitrification in the December 2011 Arctic stratosphere. Atmospheric Chemistry and Physics, 2016, 16, 9505-9532.	1.9	12
43	Synergy between middle infrared and millimeter-wave limb sounding of atmospheric temperature and minor constituents. Atmospheric Measurement Techniques, 2016, 9, 2267-2289.	1.2	8
44	A multi-wavelength classification method for polar stratospheric cloud types using infrared limb spectra. Atmospheric Measurement Techniques, 2016, 9, 3619-3639.	1.2	21
45	Tropical sources and sinks of carbonyl sulfide observed from space. Geophysical Research Letters, 2015, 42, 10,082.	1.5	44
46	Threeâ€dimensional distribution of a major desert dust outbreak over East Asia in March 2008 derived from IASI satellite observations. Journal of Geophysical Research D: Atmospheres, 2015, 120, 7099-7127.	1.2	34
47	Corrigendum to "Seasonal and interannual variations of HCN amounts in the upper troposphere and lower stratosphere observed by MIPAS" published in Atmos. Chem. Phys., 15, 563–582, 2015. Atmospheric Chemistry and Physics, 2015, 15, 2487-2488.	1.9	0
48	Sulfur dioxide (SO <sub>2</sub> ) from MIPAS in the upper troposphere and lower stratosphere 2002–2012. Atmospheric Chemistry and Physics, 2015, 15, 7017-7037.	1.9	38
49	Seasonal and interannual variations in HCN amounts in the upper troposphere and lower stratosphere observed by MIPAS. Atmospheric Chemistry and Physics, 2015, 15, 563-582.	1.9	21
50	New calibration noise suppression techniques for the GLORIA limb imager. Atmospheric Measurement Techniques, 2015, 8, 3147-3161.	1.2	4
51	Level 2 processing for the imaging Fourier transform spectrometer GLORIA: derivation and validation of temperature and trace gas volume mixing ratios from calibrated dynamics mode spectra. Atmospheric Measurement Techniques, 2015, 8, 2473-2489.	1.2	30
52	Validation of first chemistry mode retrieval results from the new limb-imaging FTS GLORIA with correlative MIPAS-STR observations. Atmospheric Measurement Techniques, 2015, 8, 2509-2520.	1.2	11
53	Stratospheric sulfur and its implications for radiative forcing simulated by the chemistry climate model EMAC. Journal of Geophysical Research D: Atmospheres, 2015, 120, 2103-2118.	1.2	59
54	Chlorine nitrate in the atmosphere over St. Petersburg. Izvestiya - Atmospheric and Oceanic Physics, 2015, 51, 49-56.	0.2	9

#	Article	IF	CITATIONS
55	Retrieval of three-dimensional small-scale structures in upper-tropospheric/lower-stratospheric composition as measured by GLORIA. Atmospheric Measurement Techniques, 2015, 8, 81-95.	1.2	38
56	Methane and nitrous oxide retrievals from MIPAS-ENVISAT. Atmospheric Measurement Techniques, 2015, 8, 4657-4670.	1.2	20
57	Level 0 to 1 processing of the imaging Fourier transform spectrometer GLORIA: generation of radiometrically and spectrally calibrated spectra. Atmospheric Measurement Techniques, 2014, 7, 4167-4184.	1.2	35
58	Gimballed Limb Observer for Radiance Imaging of the Atmosphere (GLORIA) scientific objectives. Atmospheric Measurement Techniques, 2014, 7, 1915-1928.	1.2	85
59	The added value of a visible channel to a geostationary thermal infrared instrument to monitor ozone for air quality. Atmospheric Measurement Techniques, 2014, 7, 2185-2201.	1.2	23
60	Instrument concept of the imaging Fourier transform spectrometer GLORIA. Atmospheric Measurement Techniques, 2014, 7, 3565-3577.	1.2	82
61	Validation of MIPAS IMK/IAA V5R_O3_224 ozone profiles. Atmospheric Measurement Techniques, 2014, 7, 3971-3987.	1.2	24
62	Scattering in infrared radiative transfer: A comparison between the spectrally averaging model JURASSIC and the line-by-line model KOPRA. Journal of Quantitative Spectroscopy and Radiative Transfer, 2013, 127, 102-118.	1.1	23
63	Satellite observation of lowermost tropospheric ozone by multispectral synergism of IASI thermal infrared and GOME-2 ultraviolet measurements over Europe. Atmospheric Chemistry and Physics, 2013, 13, 9675-9693.	1.9	97
64	The Australian bushfires of February 2009: MIPAS observations and GEM-AQ model results. Atmospheric Chemistry and Physics, 2013, 13, 1637-1658.	1.9	24
65	Corrigendum to "The Australian bushfires of February 2009: MIPAS observations and GEM-AQ model results" published in Atmos. Chem. Phys., 13, 1637–1658, 2013. Atmospheric Chemistry and Physics, 2013, 13, 4373-4373.	1.9	0
66	Sulfur dioxide (SO <sub>2</sub> ) as observed by MIPAS/Envisat: temporal development and spatial distribution at 15–45 km altitude. Atmospheric Chemistry and Physics, 2013, 13, 10405-10423.	1.9	29
67	MIPAS-STR measurements in the Arctic UTLS in winter/spring 2010: instrument characterization, retrieval and validation. Atmospheric Measurement Techniques, 2012, 5, 1205-1228.	1.2	36
68	Clobal distributions of C <sub>2</sub> H <sub>6</sub> , C <sub>2</sub> H <sub>2</sub> , HCN, and PAN retrieved from MIPAS reduced spectral resolution measurements. Atmospheric Measurement	1.2	44
69	Techniques, 2012, 5, 723-734. Fast cloud parameter retrievals of MIPAS/Envisat. Atmospheric Chemistry and Physics, 2012, 12, 7135-7164.	1.9	37
70	Global CFC-11 (CCl <sub>3</sub> F) and CFC-12 (CCl <sub>2</sub> F <sub>2</sub> ) measurements with the Michelson Interferometer for Passive Atmospheric Sounding (MIPAS): retrieval, climatologies and trends. Atmospheric Chemistry and Physics, 2012, 12, 11857-11875.	1.9	49
71	Clobal stratospheric hydrogen peroxide distribution from MIPAS-Envisat full resolution spectra compared to KASIMA model results. Atmospheric Chemistry and Physics, 2012, 12, 4923-4933.	1.9	6
72	The natural greenhouse effect of atmospheric oxygen (O <sub>2</sub> ) and nitrogen (N <sub>2</sub> ). Geophysical Research Letters, 2012, 39, .	1.5	11

#	Article	IF	CITATIONS
73	GRANADA: A Generic RAdiative traNsfer AnD non-LTE population algorithm. Journal of Quantitative Spectroscopy and Radiative Transfer, 2012, 113, 1771-1817.	1.1	60
74	Global observations of thermospheric temperature and nitric oxide from MIPAS spectra at 5.3 <i>μ</i> m. Journal of Geophysical Research, 2011, 116, n/a-n/a.	3.3	46
75	A thermal infrared instrument onboard a geostationary platform for CO and O <sub>3</sub> measurements in the lowermost troposphere: Observing System Simulation Experiments (OSSE). Atmospheric Measurement Techniques, 2011, 4, 1637-1661.	1.2	36
76	Comparison of HDO measurements from Envisat/MIPAS with observations by Odin/SMR and SCISAT/ACE-FTS. Atmospheric Measurement Techniques, 2011, 4, 1855-1874.	1.2	25
77	A geostationary thermal infrared sensor to monitor the lowermost troposphere: O <sub>3</sub> and CO retrieval studies. Atmospheric Measurement Techniques, 2011, 4, 297-317.	1.2	22
78	Corrigendum to "Tropospheric ozone from IASI: comparison of different inversion algorithms and validation with ozone sondes in the northern middle latitudes" published in Atmos. Chem. Phys., 9, 9329–9347, doi:10.5194/acp-9-9329-2009, 2009. Atmospheric Chemistry and Physics, 2010, 10, 6345-6345.	1.9	0
79	Global distribution and variability of formic acid as observed by MIPASâ€ENVISAT. Journal of Geophysical Research, 2010, 115, .	3.3	41
80	Retrieval of temperature, H <sub>2</sub> O, O <sub>3</sub> , HNO <sub>3</sub> , CH <sub>4</sub> , N <sub>2</sub> O, ClONO <sub>2</sub> and ClO from MIPAS reduced resolution nominal mode limb emission measurements. Atmospheric Measurement Techniques, 2009, 2, 159-175.	1.2	215
81	The horizontal resolution of MIPAS. Atmospheric Measurement Techniques, 2009, 2, 47-54.	1.2	58
82	MIPAS reduced spectral resolution UTLS-1 mode measurements of temperature, O <sub>3</sub> , HNO <sub>3</sub> , N <sub>2</sub> O, H <sub>2</sub> O and relative humidity over ice: retrievals and comparison to MLS. Atmospheric Measurement Techniques, 2009, 2,	1.2	21
83	337-353. Validation of water vapour profiles (version 13) retrieved by the IMK/IAA scientific retrieval processor based on full resolution spectra measured by MIPAS on board Envisat. Atmospheric Measurement Techniques, 2009, 2, 379-399.	1.2	28
84	Antarctic winter tropospheric warming—the potential role of polar stratospheric clouds, a sensitivity study. Atmospheric Science Letters, 2009, 10, 262-266.	0.8	6
85	Comparison between CALIPSO and MIPAS observations of polar stratospheric clouds. Journal of Geophysical Research, 2009, 114, .	3.3	43
86	Measurements of polar mesospheric clouds in infrared emission by MIPAS/ENVISAT. Journal of Geophysical Research, 2009, 114, .	3.3	15
87	Antarctic NAT PSC belt of June 2003: Observational validation of the mountain wave seeding hypothesis. Geophysical Research Letters, 2009, 36, .	1.5	56
88	HOCl chemistry in the Antarctic Stratospheric Vortex 2002, as observed with the Michelson Interferometer for Passive Atmospheric Sounding (MIPAS). Atmospheric Chemistry and Physics, 2009, 9, 1817-1829.	1.9	14
89	Carbon monoxide distributions from the upper troposphere to the mesosphere inferred from 4.7 μm non-local thermal equilibrium emissions measured by MIPAS on Envisat. Atmospheric Chemistry and Physics, 2009, 9, 2387-2411.	1.9	77
90	Tropospheric ozone from IASI: comparison of different inversion algorithms and validation with ozone sondes in the northern middle latitudes. Atmospheric Chemistry and Physics, 2009, 9, 9329-9347.	1.9	53

#	Article	IF	CITATIONS
91	Stratospheric BrONO <sub>2</sub> observed by MIPAS. Atmospheric Chemistry and Physics, 2009, 9, 1735-1746.	1.9	26
92	Validation of ozone measurements from the Atmospheric Chemistry Experiment (ACE). Atmospheric Chemistry and Physics, 2009, 9, 287-343.	1.9	134
93	Large-scale upper tropospheric pollution observed by MIPAS HCN and C <sub>2</sub> H <sub>6</sub> global distributions. Atmospheric Chemistry and Physics, 2009, 9, 9619-9634.	1.9	34
94	Validation of NO <sub>2</sub> and NO from the Atmospheric Chemistry Experiment (ACE). Atmospheric Chemistry and Physics, 2008, 8, 5801-5841.	1.9	64
95	Retrieval of global upper tropospheric and stratospheric formaldehyde (H <sub>2</sub> CO) distributions from high-resolution MIPAS-Envisat spectra. Atmospheric Chemistry and Physics, 2008, 8, 463-470.	1.9	26
96	Validation of ACE-FTS N <sub>2</sub> O measurements. Atmospheric Chemistry and Physics, 2008, 8, 4759-4786.	1.9	76
97	Vertical profile of peroxyacetyl nitrate (PAN) from MIPAS-STR measurements over Brazil in February 2005 and its contribution to tropical UT NO <sub>y</sub> partitioning. Atmospheric Chemistry and Physics, 2008, 8, 4891-4902.	1.9	28
98	Intercomparison of ILAS-II version 1.4 and version 2 target parameters with MIPAS-Envisat measurements. Atmospheric Chemistry and Physics, 2008, 8, 825-843.	1.9	12
99	CO measurements from the ACE-FTS satellite instrument: data analysis and validation using ground-based, airborne and spaceborne observations. Atmospheric Chemistry and Physics, 2008, 8, 2569-2594.	1.9	107
100	Validation of HNO <sub>3</sub> , ClONO <sub>2</sub> , and N <sub>2</sub> O <sub>5</sub> from the Atmospheric Chemistry Experiment Fourier Transform Spectrometer (ACE-FTS). Atmospheric Chemistry	1.9	75
101	and Physics, 2008, 8, 3529-3562. Global distribution of mean age of stratospheric air from MIPAS SF <sub>6</sub> measurements. Atmospheric Chemistry and Physics, 2008, 8, 677-695.	1.9	105
102	HDO measurements with MIPAS. Atmospheric Chemistry and Physics, 2007, 7, 2601-2615.	1.9	56
103	Bias determination and precision validation of ozone profiles from MIPAS-Envisat retrieved with the IMK-IAA processor. Atmospheric Chemistry and Physics, 2007, 7, 3639-3662.	1.9	49
104	Observation of Polar Stratospheric Clouds down to the Mediterranean coast. Atmospheric Chemistry and Physics, 2007, 7, 5275-5281.	1.9	11
105	MIPAS measurements of upper tropospheric C <sub>2</sub> H <sub>6</sub> and O <sub>3</sub> during the southern hemispheric biomass burning season in 2003. Atmospheric Chemistry and Physics. 2007. 7. 5861-5872.	1.9	31
106	Validation of nitric acid retrieved by the IMK-IAA processor from MIPAS/ENVISAT measurements. Atmospheric Chemistry and Physics, 2007, 7, 721-738.	1.9	31
107	Validation of MIPAS ClONO <sub>2</sub> measurements. Atmospheric Chemistry and Physics, 2007, 7, 257-281.	1.9	65
108	Global peroxyacetyl nitrate (PAN) retrieval in the upper troposphere from limb emission spectra of the Michelson Interferometer for Passive Atmospheric Sounding (MIPAS). Atmospheric Chemistry and Physics, 2007, 7, 2775-2787.	1.9	77

#	Article	IF	CITATIONS
109	Validation of MIPAS HNO <sub>3</sub> operational data. Atmospheric Chemistry and Physics, 2007, 7, 4905-4934.	1.9	48
110	Estimating cirrus cloud properties from MIPAS data. Geophysical Research Letters, 2007, 34, .	1.5	14
111	Evidence for N2Oν34.5μm non-local thermodynamic equilibrium emission in the atmosphere. Geophysical Research Letters, 2007, 34, .	1.5	5
112	Global distributions of HO2NO2as observed by the Michelson Interferometer for Passive Atmospheric Sounding (MIPAS). Journal of Geophysical Research, 2007, 112, .	3.3	16
113	Analysis of nonlocal thermodynamic equilibrium CO 4.7μm fundamental, isotopic, and hot band emissions measured by the Michelson Interferometer for Passive Atmospheric Sounding on Envisat. Journal of Geophysical Research, 2007, 112, .	3.3	23
114	Global stratospheric HOCl distributions retrieved from infrared limb emission spectra recorded by the Michelson Interferometer for Passive Atmospheric Sounding (MIPAS). Journal of Geophysical Research, 2006, 111, .	3.3	29
115	Retrieval of stratospheric ozone profiles from MIPAS/ENVISAT limb emission spectra: a sensitivity study. Atmospheric Chemistry and Physics, 2006, 6, 2767-2781.	1.9	49
116	Spectroscopic evidence for NAT, STS, and ice in MIPAS infrared limb emission measurements of polar stratospheric clouds. Atmospheric Chemistry and Physics, 2006, 6, 1201-1219.	1.9	82
117	MIPAS detects Antarctic stratospheric belt of NAT PSCs caused by mountain waves. Atmospheric Chemistry and Physics, 2006, 6, 1221-1230.	1.9	102
118	MIPAS level 2 operational analysis. Atmospheric Chemistry and Physics, 2006, 6, 5605-5630.	1.9	174
119	Vibrationally excited ozone in the middle atmosphere. Journal of Atmospheric and Solar-Terrestrial Physics, 2006, 68, 202-212.	0.6	26
120	Comparisons of MIPAS/ENVISAT and GPS-RO/CHAMP Temperatures. , 2005, , 567-572.		1
121	Comparison of GPS/SAC-C and MIPAS/ENVISAT Temperature Profiles and Its Possible Implementation for EOS MLS Observations. , 2005, , 573-578.		3
122	Three-Dimensional Model Study of the Antarctic Ozone Hole in 2002 and Comparison with 2000. Journals of the Atmospheric Sciences, 2005, 62, 822-837.	0.6	39
123	A comparison of night-time GOMOS and MIPAS ozone profiles in the stratosphere and mesosphere. Advances in Space Research, 2005, 36, 958-966.	1.2	22
124	Comparison of single and multiple scattering approaches for the simulation of limb-emission observations in the mid-IR. Journal of Quantitative Spectroscopy and Radiative Transfer, 2005, 91, 275-285.	1.1	33
125	Ozone profiles and total column amounts derived at Izaña, Tenerife Island, from FTIR solar absorption spectra, and its validation by an intercomparison to ECC-sonde and Brewer spectrometer measurements. Journal of Quantitative Spectroscopy and Radiative Transfer, 2005, 91, 245-274.	1.1	33
126	GLObal limb Radiance Imager for the Atmosphere (GLORIA): Scientific objectives. Advances in Space Research, 2005, 36, 989-995.	1.2	68

#	Article	IF	CITATIONS
127	Retrieval of stratospheric and mesospheric O3 from high resolution MIPAS spectra at 15 and 10 μm. Advances in Space Research, 2005, 36, 943-951.	1.2	21
128	Comparisons of MIPAS/ENVISAT ozone profiles with SMR/ODIN and HALOE/UARS observations. Advances in Space Research, 2005, 36, 927-931.	1.2	9
129	Cross comparisons of O3 and NO2 measured by the atmospheric ENVISAT instruments GOMOS, MIPAS, and SCIAMACHY. Advances in Space Research, 2005, 36, 855-867.	1.2	34
130	Mixing Processes during the Antarctic Vortex Split in September–October 2002 as Inferred from Source Cas and Ozone Distributions from ENVISAT–MIPAS. Journals of the Atmospheric Sciences, 2005, 62, 787-800.	0.6	74
131	Tomographic retrieval of atmospheric parameters from infrared limb emission observations. Applied Optics, 2005, 44, 3291.	2.1	43
132	Retrieval of stratospheric NOxfrom 5.3 and 6.2 μm nonlocal thermodynamic equilibrium emissions measured by Michelson Interferometer for Passive Atmospheric Sounding (MIPAS) on Envisat. Journal of Geophysical Research, 2005, 110, .	3.3	84
133	NOyfrom Michelson Interferometer for Passive Atmospheric Sounding on Environmental Satellite during the Southern Hemisphere polar vortex split in September/October 2002. Journal of Geophysical Research, 2005, 110, .	3.3	32
134	Validation of stratospheric temperatures measured by Michelson Interferometer for Passive Atmospheric Sounding (MIPAS) on Envisat. Journal of Geophysical Research, 2005, 110, .	3.3	16
135	Longitudinal variations of temperature and ozone profiles observed by MIPAS during the Antarctic stratosphere sudden warming of 2002. Journal of Geophysical Research, 2005, 110, .	3.3	9
136	Observation of NOxenhancement and ozone depletion in the Northern and Southern Hemispheres after the October-November 2003 solar proton events. Journal of Geophysical Research, 2005, 110, .	3.3	132
137	HNO3, N2O5, and ClONO2enhancements after the October-November 2003 solar proton events. Journal of Geophysical Research, 2005, 110, .	3.3	69
138	Experimental evidence of perturbed odd hydrogen and chlorine chemistry after the October 2003 solar proton events. Journal of Geophysical Research, 2005, 110, .	3.3	55
139	Water vapor distributions measured with the Michelson Interferometer for Passive Atmospheric Sounding on board Envisat (MIPAS/Envisat). Journal of Geophysical Research, 2005, 110, .	3.3	63
140	An enhanced HNO3second maximum in the Antarctic midwinter upper stratosphere 2003. Journal of Geophysical Research, 2005, 110, .	3.3	52
141	Study on the impact of polar stratospheric clouds on high resolution mid-IR limb emission spectra. Journal of Quantitative Spectroscopy and Radiative Transfer, 2004, 83, 93-107.	1.1	39
142	First results of MIPAS/ENVISAT with operational Level 2 code. Advances in Space Research, 2004, 33, 1012-1019.	1.2	51
143	Intercomparison of retrieval codes used for the analysis of high-resolution, ground-based FTIR measurements. Journal of Quantitative Spectroscopy and Radiative Transfer, 2004, 87, 25-52.	1.1	315
144	Feasibility of measurements of water vapor and ice clouds in the tropical UT/LS region with MIPAS/Envisat. Advances in Space Research, 2004, 34, 815-819.	1.2	0

#	Article	IF	CITATIONS
145	Spaceborne ClO observations by the Michelson Interferometer for Passive Atmospheric Sounding (MIPAS) before and during the Antarctic major warming in September/October 2002. Journal of Geophysical Research, 2004, 109, .	3.3	41
146	Correction to "Very early chlorine activation and ozone loss in the Arctic winter 2002–2003― Geophysical Research Letters, 2004, 31, .	1.5	0
147	First spaceborne observations of Antarctic stratospheric ClONO2recovery: Austral spring 2002. Journal of Geophysical Research, 2004, 109, .	3.3	40
148	Stratospheric N2O5in the austral spring 2002 as retrieved from limb emission spectra recorded by the Michelson Interferometer for Passive Atmospheric Sounding (MIPAS). Journal of Geophysical Research, 2004, 109, .	3.3	25
149	Cross-validation of MIPAS/ENVISAT and GPS-RO/CHAMP temperature profiles. Journal of Geophysical Research, 2004, 109, .	3.3	27
150	The ISSWG line-by-line inter-comparison experiment. Journal of Quantitative Spectroscopy and Radiative Transfer, 2003, 77, 433-453.	1.1	62
151	Modelling of atmospheric mid-infrared radiative transfer: the AMIL2DA algorithm intercomparison experiment. Journal of Quantitative Spectroscopy and Radiative Transfer, 2003, 78, 381-407.	1.1	45
152	Very early chlorine activation and ozone loss in the Arctic winter 2002-2003. Geophysical Research Letters, 2003, 30, n/a-n/a.	1.5	19
153	Retrieval of temperature and tangent altitude pointing from limb emission spectra recorded from space by the Michelson Interferometer for Passive Atmospheric Sounding (MIPAS). Journal of Geophysical Research, 2003, 108, .	3.3	242
154	Evolution of ozone and ozone-related species over Kiruna during the SOLVE/THESEO 2000 campaign retrieved from ground-based millimeter-wave and infrared observations. Journal of Geophysical Research, 2002, 107, SOL 51-1-SOL 51-12.	3.3	18
155	Intercomparison of radiative transfer codes under non-local thermodynamic equilibrium conditions. Journal of Geophysical Research, 2002, 107, ACH 12-1.	3.3	22
156	Evidence of scattering of tropospheric radiation by PSCs in mid-IR limb emission spectra: MIPAS-B observations and KOPRA simulations. Geophysical Research Letters, 2002, 29, 119-1-119-4.	1.5	62
157	Trace gas retrieval including horizontal gradients. Advances in Space Research, 2002, 29, 1631-1636.	1.2	5
158	Sequential and joint retrieval of trace gas profiles. Advances in Space Research, 2002, 29, 1649-1654.	1.2	1
159	Sensitivity of trace gas abundances retrievals from infrared limb emission spectra to simplifying approximations in radiative transfer modelling. Journal of Quantitative Spectroscopy and Radiative Transfer, 2002, 72, 249-280.	1.1	148
160	Mountain polar stratospheric cloud measurements by Ground Based FTIR Solar Absorption Spectroscopy. Geophysical Research Letters, 2001, 28, 2189-2192.	1.5	14
161	A new non-LTE retrieval method for atmospheric parameters from mipas-envisat emission spectra. Advances in Space Research, 2001, 27, 1099-1104.	1.2	49
162	Non-LTE state distribution of nitric oxide and its impact on the retrieval of the stratospheric daytime no profile from MIPAS limb sounding instruments. Advances in Space Research, 2000, 26, 947-950.	1.2	8

#	Article	IF	CITATIONS
163	Optimized forward model and retrieval scheme for MIPAS near-real-time data processing. Applied Optics, 2000, 39, 1323.	2.1	188
164	Performances of the Near Real Time Code for MIPAS Data Analysis. , 2000, , 335-347.		0
165	Efficient line-by-line calculation of absorption coefficients. Journal of Quantitative Spectroscopy and Radiative Transfer, 1999, 63, 97-114.	1.1	53
166	Atmospheric ray path modeling for radiative transfer algorithms. Applied Optics, 1999, 38, 3129.	2.1	30
167	HNO3 and PSC Measurements from the Transall: Sequestering of HNO3 in the Winter of 1994/95. Journal of Atmospheric Chemistry, 1998, 30, 61-79.	1.4	6
168	Aircraft-borne detection of stratospheric column amounts of O3, NO2, OClO, ClNO3, HNO3, and aerosols around the arctic vortex (79°N to 39°N) during spring 1993: 1. Observational data. Journal of Geophysical Research, 1997, 102, 10801-10814.	3.3	11
169	Evidence for the removal of gaseous HNO3inside the arctic polar vortex in January 1992. Geophysical Research Letters, 1996, 23, 149-152.	1.5	8
170	Correction of phase anomalies of atmospheric emission spectra by the double-differencing method. Applied Optics, 1996, 35, 2649.	2.1	10
171	The variability of ClONO2and HNO3in the Arctic polar vortex: Comparison of Transall Michelson interferometer for passive atmospheric sounding measurements and three-dimensional model results. Journal of Geophysical Research, 1995, 100, 9115.	3.3	33
172	Spatial and temporal variability of ClONO2, HNO3, and O3in the Arctic winter of 1992/1993 as obtained by airborne infrared emission spectroscopy. Journal of Geophysical Research, 1995, 100, 9101.	3.3	34
173	Airborne measurements during the European Arctic Stratospheric Ozone Experiment column amounts of HNO3and O3derived from FTIR emission sounding. Geophysical Research Letters, 1994, 21, 1351-1354.	1.5	14
174	Phase corrections for the emission sounder MIPAS-FT. Applied Optics, 1993, 32, 4586.	2.1	20
175	Characterization of the surface structure of silver single crystal electrodes by ex situ and in situ STM. Surface Science, 1992, 271, 191-200.	0.8	31
176	STM studies of real and quasi-perfect silver single crystal surfaces used in electrochemical experiments. Surface Science, 1991, 248, 225-233.	0.8	52
177	New aspects in underpotential-overpotential transitions in metal deposition processes. Surface Science, 1991, 248, 234-240.	0.8	21